Journal of Photochemistry and Photobiology A: Chemistry 200 (2008) 148–160

Contents lists available at ScienceDirect

Journal of Photochemistry and Photobiology A: Chemistry

journal homepage: www.elsevier.com/locate/jphotochem

Spectroscopy and photophysics of dimethyl-substituted alloxazines

Marek Sikorski[a,*], Dorota Prukała[a], Małgorzata Insińska-Rak[a], Igor Khmelinskii[b], David R. Worrall[c], Sian L. Williams[c], Jordi Hernando[d], Jose L. Bourdelande[d], Jacek Koput[a], Ewa Sikorska[e]

[a] Faculty of Chemistry, A. Mickiewicz University, Grunwaldzka 6, 60-780 Poznań, Poland
[b] Universidade do Algarve, FCT, Campus de Gambelas, 8005-139 Faro, Portugal
[c] Department of Chemistry, Loughborough University, Leicestershire LE11 3TU, UK
[d] Unitat de Química Orgànica, Universitat Autònoma de Barcelona, Bellaterra, Barcelona 08193, Spain
[e] Faculty of Commodity Science, The Poznań University of Economics, al. Niepodległości 10, 60-967 Poznań, Poland

ARTICLE INFO

Article history:
Received 27 February 2008
Received in revised form 17 June 2008
Accepted 4 July 2008
Available online 22 July 2008

Keywords:
Alloxazine
Lumichrome
Photochemistry
Singlet oxygen
DFT
Transient spectra
Fluorescence

ABSTRACT

We have calculated the electronic structure and absorption spectra from the ground state and the first triplet excited state for five dimethylalloxazines, using the TD-DFT approach. The results of the calculations were correlated to experimental spectral and photophysical data, including the transient spectra reported here containing triplet–triplet absorption data, using the proximity effect theory to explain the variations of the ISC rates with the substitution pattern and solvent. Additionally, singlet oxygen yields were measured for these compounds, demonstrating their high efficiency as singlet oxygen photosensitizers.

1. Introduction

The term 'flavins' refers to the 10-substituted 7,8-dimethyl-2,3,4,10-tetrahydro-benzo[*g*]pteridine-2,4-diones, lumiflavin (7,8,10-trimethyl-10*H*-benzo[*g*]pteridine-2,4-dione) being the parent molecule from which all other variants derive, *e.g.*, vitamin B_2 (riboflavin), flavin mononucleotide (FMN) and flavin adenine dinucleotide (FAD). The motivation behind the large effort put into flavin studies over a number of years comes from the realization that the excited states of flavins play an important role in living organisms and are involved in a number of important photobiological and photochemical processes, such as phototropism, phototaxis, and photodynamic action. The photochemistry of isoalloxazines (10-substituted 2,3,4,10-tetrahydro-benzo[*g*]pteridine-2,4-diones), and especially the photochemistry of flavins (7,8-dimethyl-substituted isoalloxazines) has been the subject of intense research over the years [1].

In contrast to flavins, the closely related alloxazines (benzo[*g*]pteridine-2,4(1*H*,3*H*)-diones) have received relatively little attention. The major aspects of the spectroscopy of alloxazines in their singlet states are understood fairly well, but, with the exception of our own recent studies [2–6], the published data were mostly limited to steady-state measurements of absorption and fluorescence [7]. The early interest in the spectral and photophysical properties of alloxazines, including lumichrome (7,8-dimethylalloxazine = 7,8-dimethylbenzo[*g*]pteridine-2,4(1*H*,3*H*)-dione), was driven mainly by their similarity to isoalloxazines and in particular to flavins. They were also the subject of interest as photodecomposition products of flavins. Some of the interest in alloxazines has been driven by the discovery of excited-state double proton transfer (ESDPT) in lumichrome in the presence of acetic acid [8,9]. Alloxazines and related compounds belong to an interesting group of species whose hydrogen-bonded complexes are capable of undergoing ESDPT; we have examined the mechanism of photo-initiated double proton transfer for a set of differently substituted methyl- and cyanoalloxazines in 1,2-dichloroethane [10]. In a more detailed recent study, we have investigated the photoinduced proton transfer of lumichrome in the presence of acetic acid in 1,2-dichloroethane, acetonitrile and pure acetic acid [11–14]. Presently, the interest in

* Corresponding author. Tel.: +48 61 8291309; fax: +48 61 8658008.
E-mail address: sikorski@amu.edu.pl (M. Sikorski).

1010-6030/$ – see front matter © 2008 Elsevier B.V. All rights reserved.
doi:10.1016/j.jphotochem.2008.07.006

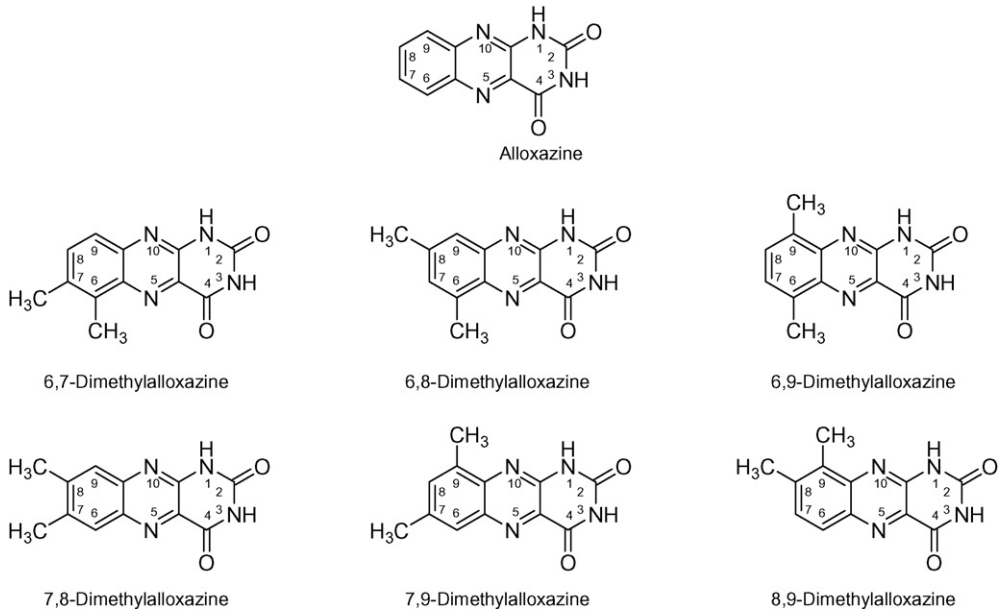

Fig. 1. Structure of alloxazines and their atom numbering.

alloxazines is a focal point of a growing body of research, motivated by remarkable new findings, and discoveries of promising practical applications of alloxazines, described below.

To give some examples of the important findings of recent years, we shall note that lumichrome has been identified as the first natural metamorphosis-inducing substance in ascidians [15,16]. In contrast, riboflavin, a possible parent compound of lumichrome, has been found inactive in induction of larval metamorphosis. It has been shown that *Sinorhizobium meliloti* bacteria produce lumichrome that enhances root respiration in alfalfa (*Medicago sativa* L.) and also triggers a compensatory increase in whole-plant net carbon assimilation [17]. The well-known rapid degradation of riboflavin to lumichrome under many physiological conditions and the prevalence of riboflavin release by rhizosphere bacteria suggest that the events demonstrated in the *S. meliloti*-alfalfa association may be widely important across many plant-microbe interactions.

Some other interesting facts, which have increased the recent interest in alloxazines, include an important conclusion of our studies that alloxazines and lumichromes are efficient singlet oxygen photosensitizers [18–20]. Alloxazine nucleosides are potentially of interest as fluorescent probes and have been predicted to exhibit hydrogen-bonding characteristics similar to those of thymidine [21]. Recently, it has been proposed that alloxazines may play an important role in the photodegradation of polyamidehydroxyurethane polymers in aqueous solution, and that singlet oxygen may be involved in the process [22]. High-quality alloxazine-imprinted polymers have been prepared and proposed for application in HPLC analysis [23]. Remarkably, strong binding

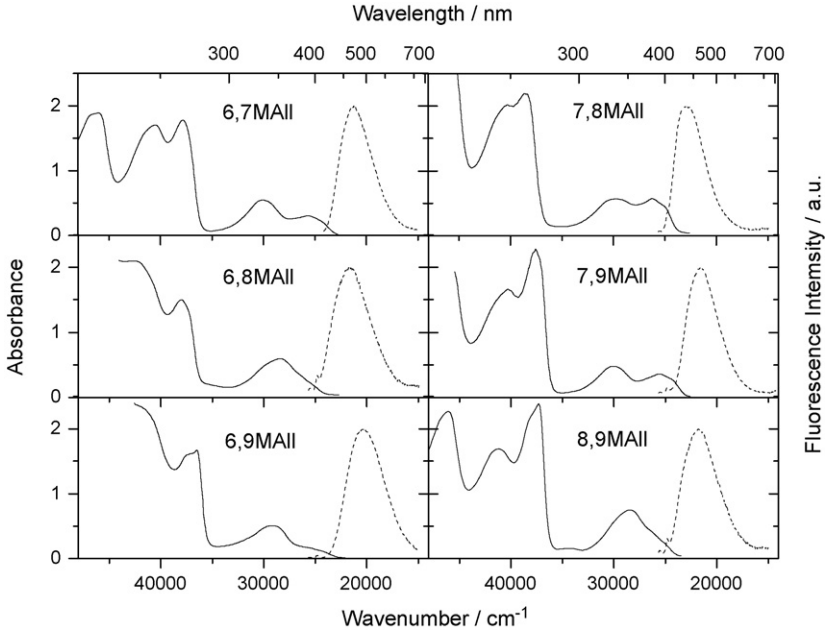

Fig. 2. Absorption (solid line) and fluorescence (dashed line) spectra of dimethylalloxazines in acetonitrile solutions.

Table 1
Spectroscopic and photophysical data for the singlet states of alloxazine and its dimethyl-substituted derivatives[a]

Solvent	Compound	λ_2 (nm)	λ_1 (nm)	λ_F (nm)	ϕ_F	τ_F (ns)	k_r ($\times 10^8$ s^{-1})	Σk_{nr} ($\times 10^8$ s^{-1})
1,4-Dioxane	All	318	372	435				
	6,7MAll[b]	331	387	468	0.025	1.0	0.25	9.8
	6,8MAll[c]	350		462	0.016	0.70	0.22	14
	6,9MAll	346	382	469	0.036	2.1	0.17	4.6
	7,8MAll[d]	327	379	428	0.026	0.45	0.58	22
	7,9MAll	330	380	451	0.030	0.94	0.32	10
	8,9MAll	348	376[e]	442	0.016	0.59	0.27	17
1,2-Dichloroethane	All	322	374	434	0.023	0.19	1.2	51
	6,7MAll[b]	335	380	468	0.038	2.18	0.17	4.4
	6,8MAll[c]	350		463	0.017	1.19	0.14	8.3
	6,9MAll	344	380	491	0.094	9.49	0.10	0.95
	7,8MAll[d]	322	374	434	0.023	0.19	1.2	51
	7,9MAll	333	379	465	0.041	1.58	0.26	6.1
	8,9MAll	351	375[e]	462	0.017	1.02	0.17	9.6
Acetonitrile	All	320	372	432	0.009	0.35	0.26	28
	6,7MAll[b]	332	391	469	0.041	2.41	0.17	4.0
	6,8MAll[c]	350		461	0.020	1.24	0.16	7.9
	6,9MAll	343	388	491	0.080	8.88	0.09	1.0
	7,8MAll[d]	334	384	436	0.028	0.64	0.43	15.2
	7,9MAll	330	388	463	0.043	1.65	0.26	5.8
	8,9MAll	351	375[e]	461	0.019	1.14	0.16	6.1
Methanol	6,7MAll[b]	335	391	486	0.075	4.2	0.18	2.2
	6,8MAll[c]	352		475	0.034	2.28	0.15	4.2
	6,9MAll	347	388	513	0.12	11.7	0.10	0.8
	7,8MAll[d]	339	384	461	0.032	1.04	0.30	9.3
	7,9MAll	333	389	476	0.10	3.7	0.27	2.4
	8,9MAll	354	383[e]	473	0.039	2.41	0.16	4.0

[a] λ_1, λ_2 Are the positions of the two lowest-energy bands in the absorption spectra, λ_F is the fluorescence emission maximum, ϕ_F is the fluorescence quantum yield, τ_F is the fluorescence lifetime, k_r is the radiative rate constant, and Σk_{nr} is the sum of non-radiative rate constants.
[b] From Ref. [5].
[c] From Ref. [4].
[d] From Ref. [47].
[e] Obtained by fitting Gaussians to the two lowest-energy bands.

of lumichrome to fluoride and acetate anions has been discovered and therefore proposed to be used as a new fluorescence probe for these two anions [24]. Encinas et al. [25,26] studied the electron-transfer reactions of lumichrome in methanol. Recent studies by Corbin [27,28] suggest that riboflavin and lumichrome, which have extremely good safety profiles, can inactivate high levels of a broad range of viruses and bacteria in platelet concentrates, fresh frozen plasma, and in red blood cells. One of the interesting applications of lumichrome is its use in an optical transistor device fabricated using a thin film of lumichrome on a conductive SnO_2 glass [29].

In recent years we have dedicated a lot of our attention to studies of alloxazines in solution [2,3,5,6,10,11,18–20,30,31] and in

Table 2
The lowest predicted (B3LYP/6-31G(d)) $S_0 \rightarrow S_i$ excitation energies with their corresponding oscillator strengths, f

$S_0 \rightarrow S_i$	6,7-Dimethylalloxazine[a]		6,8-Dimethylalloxazine[b]		6,9-Dimethylalloxazine		7,9-Dimethylalloxazine		8,9-Dimethylalloxazine	
	E ($\times 10^{-3}$ cm^{-1})	f	E ($\times 10^{-3}$ cm^{-1})	f	E ($\times 10^{-3}$ cm^{-1})	f	E ($\times 10^{-3}$ cm^{-1})	f	E ($\times 10^{-3}$ cm^{-1})	f
$\rightarrow S_1$	26.4	0.038	27.6	0.002	26.2	0.031	26.9	0.054	27.2	0.027
	26.3				**26.3**		**26.4**		**26.6**	
$\rightarrow S_2$	27.4	0.002	27.6	0.025	27.4	0.001	27.5	0.002	27.5	0.002
$\rightarrow S_3$	31.6	0.164	30.9	0.217	31.1	0.154	31.8	0.135	30.9	0.206
	29.8		**28.6**		**29.1**		**30.0**		**28.5**	
$\rightarrow S_4$	31.9	<0.001	32.0	<0.001	31.9	<0.001	32.0	<0.001	31.9	<0.001
$\rightarrow S_5$	38.6	0.024	38.7	0.008	38.6	0.048	38.6	0.044	38.6	0.011
$\rightarrow S_6$	39.0	0	39.0	0	38.9	0	38.9	0	39.0	0
$\rightarrow S_7$	39.7	<0.001	39.6	0	39.2	0.363	39.6	0	39.7	0
$\rightarrow S_8$	39.7	0.318	39.9	0.263	39.5	0	39.8	0.461	40.3	0.428
$\rightarrow S_9$	40.8	0	41.2	0	40.9	0	41.2	<0.001	40.8	<0.001
$\rightarrow S_{10}$	42.7	0.245	42.2	0.103	42.5	0.094	42.3	0.181	42.4	0.144
$\rightarrow S_{11}$	43.0	0.482	43.3	0.679	43.7	0.399	43.2	0.355	43.4	0.452
$\rightarrow S_{12}$	45.0	<0.001	44.6	<0.001	44.6	<0.001	44.5	<0.001	44.8	<0.001
$\rightarrow S_{13}$	47.4	0.068	47.9	0	47.4	0.081	47.5	0.059	47.7	0.076
$\rightarrow S_{14}$	47.9	<0.001	48.3	0.055	47.9	0	47.9	0	47.9	<0.001
$\rightarrow S_{15}$	49.5	<0.001	49.8	0.009	49.9	0.014	49.8	0.031	49.5	<0.001

Experimental values taken in 1,2-dichloroethane solutions are listed in bold type for comparison.
[a] From Ref. [5].
[b] From Ref. [4].

Table 3
The lowest predicted (UB3LYP/6-31G(d)) $T_1 \rightarrow T_i$ excitation energies with their corresponding oscillator strengths, f[a]

$T_1 \rightarrow T_i$	6,7-Dimethylalloxazine[b]		6,8-Dimethylalloxazine[c]		6,9-Dimethylalloxazine		7,9-Dimethylalloxazine		8,9-Dimethylalloxazine	
	E ($\times 10^{-3}$ cm^{-1})	f	E ($\times 10^{-3}$ cm^{-1})	f	E ($\times 10^{-3}$ cm^{-1})	f	E ($\times 10^{-3}$ cm^{-1})	f	E ($\times 10^{-3}$ cm^{-1})	f
$\rightarrow T_2$	8.3	0.008	6.8	0.003	8.5	0.007	8.3	0	7.2	0.007
$\rightarrow T_3$	8.2	0	7.9	0	8.8	0	8.5	0.009	8.0	0
$\rightarrow T_4$	12.8	0	12.1	0	13.2	0	13.1	0	12.4	0
$\rightarrow T_5$	14.8	0.004	15.6	0.005	15.3	0.007	14.9	0.010	15.8	0.009
$\rightarrow T_6$	17.3	0.004	16.7	0.001	17.6	<0.001	17.6	0.002	17.0	<0.001
$\rightarrow T_7$	17.9	0.004	18.2	<0.001	18.3	0.004	18.2	0.001	18.1	0.003
$\rightarrow T_8$	19.5	<0.001	19.4	<0.001	20.0	<0.001	19.8	<0.001	19.3	<0.001
$\rightarrow T_9$	20.7	0	19.6	0.051	21.0	0	21.0	0	20.2	0.036
			19.2						**19.2**	
$\rightarrow T_{10}$	21.1	0.107	20.0	<0.001	21.3	0.059	21.1	0.085	20.3	0
	20.0				**20.4**		**20.0**			
$\rightarrow T_{11}$	25.6	0.041	25.0	0.057	25.4	0.060	25.1	0.078	24.8	0.084
			23.2				**22.7**		**22.2**	
$\rightarrow T_{12}$	27.3	<0.001	27.0	<0.001	27.2	<0.001	27.3	<0.001	27.2	<0.001
$\rightarrow T_{13}$	28.3	0.037	28.7	0.065	28.4	0.037	28.3	0.028	28.6	0.029
$\rightarrow T_{14}$	30.2	0	29.6	0	29.9	0	30.3	0	29.9	0
$\rightarrow T_{15}$	31.3	0.265	30.5	0.226	31.2	0.254	31.5	0.368	31.2	0.368
	27.8		**27.0**		**27.7**		**27.8**		**27.8**	
$\rightarrow T_{16}$	32.6	0	32.4	0.167	32.8	0.090	33.0	0.089	32.7	0

Experimental values taken in acetonitrile are listed in bold type for comparison.
[a] The energy of the first triplet state is as follows: 18 200, 18 900, 18 200, 18 200, and 18 600 cm^{-1} for 6,7MAll, 6,8MAll, 6,9MAll, 7,9MAll and 8,9MAll, respectively. All energies were calculated using the unrestricted formalism (UB3LYP/6-31G*).
[b] From Ref. [5].
[c] From Ref. [4].

solids [32–38]. Widely studied were alloxazine and its variously substituted monomethyl- and cyano-derivatives with the respective group in positions 6, 7, 8, or 9. Much less attention, with an important exception of lumichrome (7,8-dimethylalloxazine), has been paid to other dimethyl-substituted alloxazines. As a result, the available information on the spectroscopy and photophysics of dimethylalloxazine derivatives other than lumichrome is rather incomplete [5,6,31,38]; previous studies of these compounds were focused mostly on their steady-state emission and absorption spectroscopy and properties in heterogeneous environments, such as cellulose or crystal powders [39]. Still, even based on those early studies, one would expect the existence of some interesting properties in this class of compounds. The aim of the present paper is to characterize and reconcile the diverse data on photophysical and spectroscopic properties of dimethyl-substituted alloxazines, and to use time-dependent density-functional theory (TD-DFT) calculations to correlate changes in the electronic structure with the substitution patterns. The structures and abbreviations of the dimethylalloxazines studied here are presented in Fig. 1.

2. Experimental

The solvents acetonitrile, 1,2-dichloroethane, 1,4-dioxane, ethanol, and methanol, all from Aldrich, were used as received. Acetonitrile was dried by refluxing over calcium hydride immediately

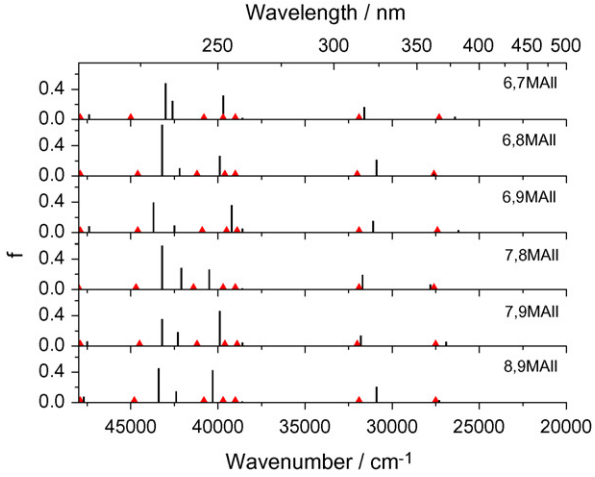

Fig. 3. Predicted $S_0 \rightarrow S_i$ transitions in dimethylalloxazines obtained in the DFT (B3LYP/6-31G(d)) calculations. Transition energies and oscillator strengths (f) are indicated by solid vertical bars. Triangles mark the weak n,π^* transitions.

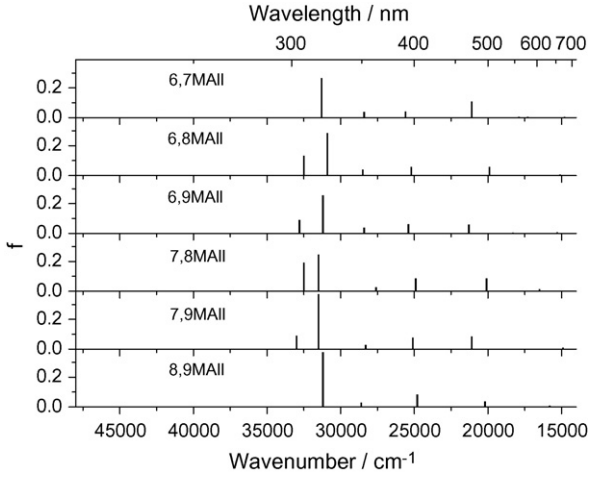

Fig. 4. Predicted $T_1 \rightarrow T_i$ transitions in dimethylalloxazines obtained in the DFT (UB3LYP/6-31G(d)) calculations: calculated triplet excitation energies, E, starting from the lowest triplet state and the corresponding oscillator strengths, f.

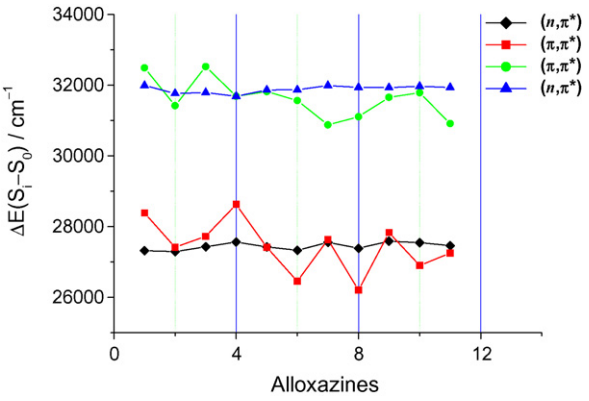

Fig. 5. Predicted lowest singlet–singlet transitions of alloxazines. Numbering of compounds: (1) alloxazine, (2) 6-methylalloxazine, (3) 7-methylalloxazine, (4) 8-methylalloxazine, (5) 9-methylalloxazine, (6) 6,7-dimethylalloxazine, (7) 6,8-dimethylalloxazine, (8) 6,9-dimethylalloxazine, (9) 7,8-dimethylalloxazine, (10) 7,9-dimethylalloxazine, and (11) 8,9-dimethylalloxazine.

before use. The dimethylalloxazines were prepared according to reference [7].

All experiments were carried out at room temperature. UV–vis absorption and fluorescence spectra were recorded, respectively, on a Varian Cary 5E spectrophotometer and a Jobin Yvon-Spex Fluorolog 3-11 spectrofluorometer. All fluorescence spectra were corrected for instrumental factors by means of a Rhodamine B quantum counter and correction files supplied by the manufacturer. Fluorescence quantum yields were measured relative to quinine sulphate in 0.1N H_2SO_4 ($\phi_F = 0.52$) as standard [40]. Fluorescence lifetimes were determined using excitation at 355 nm and by single-photon timing using a commercially available, IBH model 5000U spectrometer equipped with a hydrogen-filled nanosecond flash-lamp and the analysis software supplied by the manufacturer. Theoretical equations were fitted to experimental data by means of a nonlinear weighted least-squares routine based on the Marquardt algorithm.

In transient absorption experiments, LKS60 nanosecond laser flash photolysis instrument from Applied Photophysics available in Barcelona has been used with right-angle geometry. The third harmonic (355 nm) of a Q-switched Nd:YAG laser (Spectron Laser Systems, UK; pulse width *ca.* 9 ns) was employed for laser flash excitation. Unless otherwise indicated, the samples were purged with nitrogen.

Singlet oxygen luminescence experiments were carried out using the third harmonic (355 nm) of a Nd:YAG laser (Lumonics hyperYAG HY200, 8 mJ/pulse, *ca.* 8 ns FWHM) as the excitation source. The laser pulse energy was attenuated using solutions of sodium nitrite in water. Singlet oxygen emission at 1270 nm was measured with liquid-nitrogen-cooled *North Coast Scientific* EO-980P Ge photodiode detector. The luminescence was detected after passing through a *Melles Griot* interference filter. Data capture was with a 250MS/s digitising oscilloscope (Tektronix 2432A). Perinaphthenone (Aldrich) was used as a reference for singlet oxygen quantum yield, $\phi_\Delta = 0.95 \pm 0.05$ [41].

3. Theoretical procedures

The electronic structure of dimethylalloxazines have been studied by means of time-dependent density functional theory [42]. In this work, the TD-DFT calculations were performed using the B3LYP functional [43] in conjunction with a modest 6-31G* split-valence polarized basis set [44], and also using the conductor polarizable continuum model (CPCM) [45] to include bulk solvent effects. Excitation energies and oscillator strengths in the dipole length representation were computed using the B3LYP functional in connection with time dependent (TD) approach as implemented

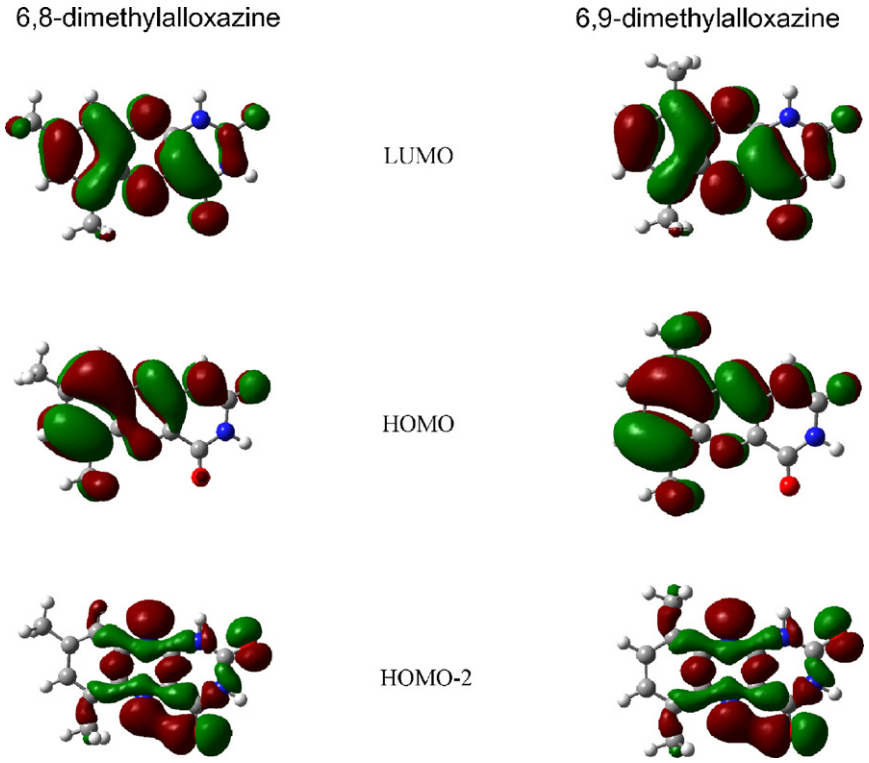

Fig. 6. The shape of the highest occupied molecular orbitals (HOMO) and the lowest unoccupied molecular orbitals (LUMO) of 6,8-dimethylalloxazine and 6,9-dimethylalloxazine, mainly involved in the lowest singlet–singlet transitions. The isosurfaces correspond to the wave function value of ±0.02.

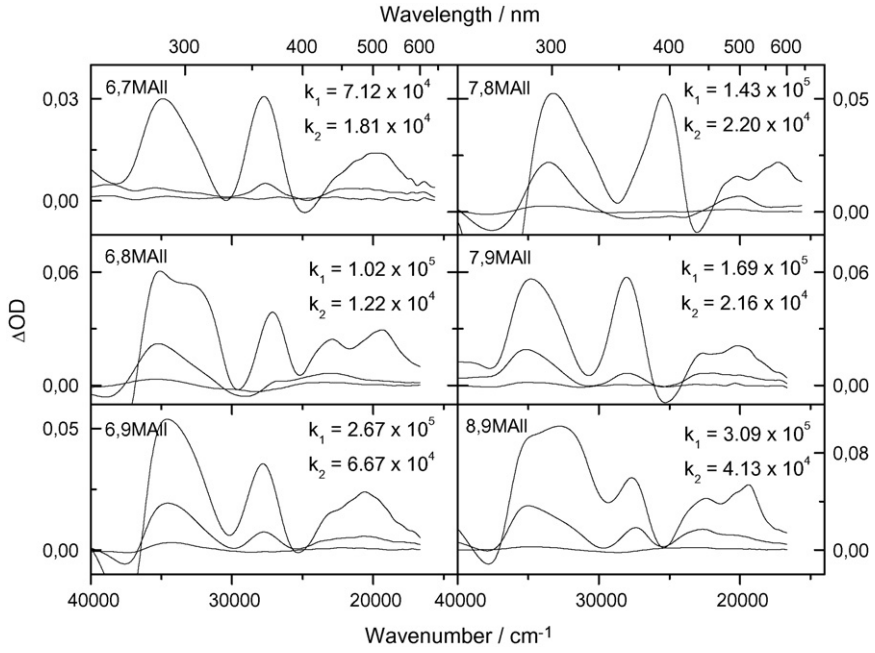

Fig. 7. Experimental transient absorption spectra of dimethylalloxazines in acetonitrile excited at 355 nm, using (6,7MAll OD_{355} = 0.293, 6,8MAll OD_{355} = 0.398, 6,9MAll OD_{355} = 0.402, 7,8MAll OD_{355} = 0.308, 7,9MAll OD_{355} = 0.402, and 8,9MAll OD_{355} = 0.405), 2 mJ/pulse, l = 1 cm.

in the Gaussian 03 package of *ab initio* programs [46]. Predicted lowest-energy singlet–singlet $S_0 \rightarrow S_i$ transitions as well as spin-forbidden $S_0 \rightarrow T_i$ transitions in alloxazines were calculated for the optimized ground-state geometry, whereas $T_1 \rightarrow T_i$ excitation energies and transition intensities were determined for the optimized geometry of the lowest triplet state (T_1), using the unrestricted UB3LYP method suitable for open-shell systems. The geometry optimization was followed by vibrational frequency calculations to verify the type of the minimum located, which revealed no imaginary frequencies. No attempt was made to locate alternative minima starting from different initial structures. Regarding the quality of the spectral predictions, we shall just note that the difference in the experimental transition energies in 1,4-dioxane solution between lumiflavin and lumichrome (22.7×10^3 cm^{-1} and 26.4×10^3 cm^{-1}) is reproduced in the calculations (24.5×10^3 cm^{-1} and 27.8×10^3 cm^{-1}) to within 0.5×10^3 cm^{-1} [47]. As had been verified previously [2,47,48], the theoretical approaches implemented are sufficient for the present purposes, with additional improvements either irrelevant or currently unfeasible.

Two different approaches were tested to account for solvent effects. The first approach included the bulk (macroscopic) solvent effects (acetonitrile or water) accounted for in the calculations by virtue of the CPCM model. Two representative alloxazines were chosen for these tests, alloxazine itself and 6,9-dimethylalloxazine. These two molecules differ significantly in their experimental spectral and photophysical properties, and also in the properties of their excited states as predicted by conventional DFT calculations that ignore solvent effects. Note that solvent effect calculations have been previously reported for lumichrome, where methanol and acetic acid molecules were added at different locations all around the lumichrome molecule, in order to study the resulting hydrogen-bond complexes of lumichrome with methanol or acetic acid [13].

The second approach was used to test the effect of specific (microscopic) solvent effects on the absorption spectra of alloxazines, that are omitted in the CPCM calculations. In the supermolecule model used to quantify the interactions between 6,9-dimethylalloxazine and water, a single water molecule was added to a 6,9-dimethylalloxazine molecule at the locations considered important for hydrogen bond formation. The corresponding optimized structures may be used as models for aqueous 6,9-dimethylalloxazine. The model used is necessarily simplified because in reality many molecules of solvent are present, thus it would be necessary to average over all possible configurations of the solvent molecules taking into account their respective Boltzmann probabilities.

4. Results and discussion

4.1. Absorption spectra

All of the dimethylalloxazines studied in this paper exhibit absorption spectra with several major bands in the UV–visible region, see Fig. 2. Typically alloxazines exhibit a spectrum with two well-separated bands at longer wavelengths, the two long-wavelength maxima in, *e.g.*, 7,8-dimethylalloxazine are at about 322 and 374 nm in dichloroethane, 334 and 384 nm in acetonitrile and 339 and 384 nm in methanol (see Table 1). However, the absorption spectrum of some dimethylalloxazines in the near–UV region shows one broad band only at approximately 350 nm, as is the case in, for example, 6,8-dimethylalloxazine and 8,9-dimethylalloxazine. However, as we will show later, the two lowest-energy transitions in fact overlap in these compounds, and show up as a single broad band. Polarization spectroscopy has been used by Song et al. [49] and by us [50] to show that the two observed absorption maxima (usually well separated) are related to two independent π,π^* transitions. However, we found that each of these lowest-energy π,π^* transitions is accompanied by a closely lying n,π^* transition. The positions of these lowest-energy absorption bands in the solvents examined are listed in Table 1, with the corresponding spectra shown in Fig. 2. As can be seen from the data of Table 1, the positions of the lowest-energy bands are not much affected by polarity or the hydrogen-bond donating ability of the solvent (*vide supra*). The observation of very similar positions of the absorption bands in polar acetonitrile and non-polar 1,2-dichloroethane gives support to the observation that the solvent polarity affects the band positions only weakly, if at all.

Table 4
Triplet state lifetimes, τ_T, quantum yields of photosensitized production of singlet oxygen, ϕ_Δ, and singlet oxygen lifetimes, τ_Δ, for alloxazine and its dimethyl-substituted derivatives in acetonitrile solutions

Compound	τ_T (μs)	k_{N_2} ($\times 10^4$ s^{-1})	k_{Air} ($\times 10^6$ s^{-1})	ϕ_Δ	τ_Δ (μs)
Alloxazine[a]	10	10.0		0.41	
6,7-Dimethylalloxazine	14	7.12	3.13	0.88	76
6,8-Dimethylalloxazine	22	4.55	2.23	0.91	79
6,9-Dimethylalloxazine	12	8.23	3.86	0.85	80
7,8-Dimethylalloxazine[a]	11	9.09		0.73	75
7,9-Dimethylalloxazine	20	5.11	3.4	0.86	80
8,9-Dimethylalloxazine	13	7.94	2.82	0.81	78

The rate constants with and without the presence of air are given, providing an estimate of the quenching rate constant. For most of the compounds, except lumichrome, the ISC quantum yield has not been determined.
[a] From Ref. [18].

The effect of the position of the methyl substituent on the spectral and photophysical properties of methyl-substituted alloxazines is, in our opinion, much more pronounced and interesting than the solvent effect. The effect of introducing a single methyl group into the alloxazine benzene ring has been the subject of a previous study [2]. Methyl substitution induces changes in the spectral properties as compared to the parent molecule, alloxazine. These changes include a distinct shift in the positions of maxima and a change in the band shapes of the absorption spectra. Alloxazine itself exhibits an absorption spectrum with two well-separated bands at longer wavelengths, with two lower-energy maxima in, *e.g.*, 1,2-dichloroethane at about 322 and 374 nm. Methyl substitution at positions 6 or 9 causes a very similar shift of these two absorption bands to the red if compared to alloxazine. Methyl substitution at position 7 causes better separation of the two absorption bands, leaving the second band unaltered and shifting the first one to the red. In contrast to methyl substitution at position 7, methyl substitution at position 8 merges both absorption bands due to shifts in opposite directions, making them difficult to distinguish. In the case of compounds with two methyl groups in the benzene ring (namely, 6,7-, 6,8-, 6,9-, 7,8-, 7,9-, and 8,9-dimethylalloxazines) the inspection of the results presented in Table 1 reveals that in each case the spectral data reflect something close to a sum of individual effects of the methyl substituents in particular positions observed in monomethyl derivatives. In particular, 6,9-dimethylalloxazine represents the most noteworthy case, because the two effects observed with the methyl group substituted in positions 6 and 9 are additive. This effect leads to an absorption spectrum similar to those of 6,8-dimethylalloxazine and 8,9-dimethylalloxazine, with only one broad maximum at approximately 350 nm. Still, the spectral properties of each of the other dimethylalloxazines may be interpreted in terms of additive superposition of the effects of the monomethyl substitutions in the positions 6, 7, 8, and/or 9.

To learn more about the electronic structure of alloxazines, TD-DFT calculations were performed. Recently, a relatively large number of iso- and alloxazines including monomethyl-substituted iso- and alloxazines, and di-, tri-, and tetra-methylisoalloxazines have been studied using similar TD-DFT calculations for singlet and triplet absorption spectra [2,4,5,31,47,51–54]. Earlier it has been shown that our results for lumiflavins are consistent and agree well with those published recently by Neiss et al. [51,55]. Both the results by Neiss et al. and our recent results for iso- and alloxazines demonstrate some very encouraging improvements as compared to previous semi-empirical and *ab initio* calculations [49,56]. In particular, the present results succeeded in reproducing the correct order of the expected singlet excited states and oscillator strengths of the respective transitions. However, as always when making comparison of the properties predicted in calculations of isolated molecules to those measured in a real solvent, we would primarily like to consider the order of the excited states and the trends, which are well noticeable when one compares a large number of closely related iso- and alloxazines. In this context the present paper concludes our studies of the effect of methyl substituent in a series of iso- and alloxazines. The TD-DFT results are presented in Tables 2 and 3 and in Figs. 3–5.

Here we have to correct a misstatement, which is not limited to our own papers, see for example [51]. In some of our previous works on isoalloxazines and alloxazines, we stated that "To the best of our knowledge, there are no published experimental gas-phase spectra for the compounds examined in our studies". Now, and with full credits to Prof. F. Müller [57], we can correct this, noting that experimental gas-phase spectra have been published in several papers [58–60].

As typical for alloxazine derivatives, π,π* transitions are accompanied by closely located n,π* transitions. On the basis of the data in Table 2, the calculated energy separation between the first two singlet states $E_{n,\pi^*} - E_{\pi,\pi^*}$ is such that the two states can be considered isoenergetic, with the exception of 6,7-dimethyl- and 6,9-dimethylalloxazines. However, even for those two derivatives the calculated energy separation of the two singlet states $E_{n,\pi^*} - E_{\pi,\pi^*}$ is still below 1200 cm^{-1}. There is an effect of the methyl group position on the energy of the absorption maxima, reproduced relatively well by the theoretical predictions presented in Fig. 3 and Table 2. Another interesting comparison and relatively good correlation of the experimental and theoretical predictions can be seen for 6,8-dimethylalloxazine and 8,9-dimethylalloxazine. Experimentally, we see a single maximum for each of these molecules with a shoulder, indicating the presence of two closely spaced π,π* transitions. This is also reflected in the calculations where the two predicted π,π* transitions shift closer to each other.

In alloxazines, as is the case of many aza-aromatics, close-neighbouring n,π* and π,π* singlet excited states (calculated $\Delta E < 1200$ cm^{-1}) lead to the so-called *proximity effect* [61]. The proximity effect is believed to be a consequence of vibronic interaction between the lowest n,π* and π,π* singlet states, where these lie close together in energy. In such cases, this vibronic coupling can be used to rationalize the photophysical properties of alloxazines. As mentioned earlier, based on the polarization spectra Song et al. [49] proposed not only that the two states should be close in energy but also that strong vibronic coupling should exist between closely-spaced n,π* and π,π* states. Both TD-DFT calculations and experimental results presented here confirm this hypothesis. As expected with the proximity effect playing the dominant role, the radiative rate constants of alloxazines are not affected strongly by polarity or by the protic character of the solvent. In contrast to the radiative rate constant, the non-radiative rate constant does get affected by the solvent due to the proximity effect, which also varies in function of the substitution pattern and other factors.

Fig. 6 depicts the shape of the lowest unoccupied molecular orbital (LUMO) and the highest occupied molecular orbital

(HOMO), involved in the transitions to the low-lying excited states of 6,8-dimethylalloxazine and 6,9-dimethylalloxazine. For 6,7-dimethylalloxazine, 6,9-dimethylalloxazine, 7,9-dimethylalloxazine, and 8,9-dimethylalloxazine examined in this study, the $S_0 \rightarrow S_1$ transition has a dominant contribution from the HOMO→LUMO excitation and is assigned as an allowed π,π^* transition. Note that the lowest singlet excited state predicted for 6,8-dimethylalloxazine and 7,8-dimethylalloxazine has a dominant contribution from the HOMO-2 → LUMO excitation and is assigned as an n,π^* transition. However, these n,π^* transitions are accompanied by closely located π,π^* transitions with a dominant contribution from the HOMO → LUMO excitation.

Fig. 5 illustrates the substituent effects on the energy of the lowest excited singlet states, including alloxazine and its mono- and dimethyl-substituted derivatives with an extra methyl group in positions 6, 7, 8, or 9, giving a total of 11 alloxazine compounds for comparison. The results presented in Fig. 5 clearly show that the n,π^* and π,π^* singlet excited states are lying close to each other in all of the compounds examined, with $\Delta E < 1200\,cm^{-1}$. However, some trends may be noted for the molecules with methyl groups in different positions. Alloxazine and 8-methylalloxazine have the predicted n,π^* singlet state with the lowest energy. In contrast, in 6,7-dimethylalloxazine, 6,9-dimethylalloxazine, and 7,9-dimethylalloxazine the lowest excited singlet states have the π,π^* character, while in all other alloxazine derivatives the n,π^* and π,π^* singlet excited states are predicted to be virtually isoenergetic.

4.2. Transient absorption spectra

The interest in the triplet states of alloxazines was also limited mainly to lumichrome and its derivatives, with very little data published regarding the transient absorption spectra of the triplet excited states of other alloxazines. In particular, with the exception of lumichrome (7,8-dimethylalloxazine) we are aware of no reported information about the triplet–triplet spectra of dimethylalloxazines in acetonitrile or any other medium. Upon laser excitation at 355 nm, dimethylalloxazines in acetonitrile produce transient species that decay on the microsecond time scale. Transient difference spectra for dimethylalloxazines in acetonitrile are presented in Fig. 7. As shown, a negative absorbance change near 390 nm is observed for all of the dimethylalloxazines, as a result of the excited-state molar absorption coefficient being lower than that of the ground state in this range. Although the transient absorption spectra of all of the alloxazines are similar, some differences are apparent in the positions of the maxima. The spectra in Fig. 7 are similar to those previously reported for lumichrome and monomethyl-substituted alloxazines [2,32,62], which show peaks in their triplet state spectra at around 360, 440, and 520 nm. In some cases, as in 6,7-dimethylalloxazine and 6,9-dimethylalloxazine, the two latter bands have the tendency to overlap into a single band with the only maximum at about 490 nm. Note that the positions and relative intensities of the lowest-energy peaks in the triplet–triplet absorption spectra are unaffected by the ground-state depletion.

As has been reported earlier for lumichrome and mono methyl substituted alloxazines [18,63], two kinetically distinct species have been observed in the transient absorption spectra. Close inspection of the previously published data and especially of the recent study by Jiang and co-workers [64] has shown that self-quenching of triplet excited lumichrome by ground-state lumichrome molecules results in a wide absorption band at 430–530 nm, attributed to the radical anion. This attribution has been confirmed by the signal dependence on the excitation laser pulse energy, alloxazine concentration, and oxygen quenching effect. The longer-lived radical anion species was formed at the rate coinciding with the respective triplet decay rate, resulting in a clear parent/offspring relationship. These conclusions were also confirmed in the present work by successful application of global analysis to all of the studied compounds, assuming the kinetic scheme:

$$A \xrightarrow{k_1} B \xrightarrow{k_2} C \quad (1)$$

Here *A* represents the triplet excited state, *B* the longer-lived transient species (anion radical), and *C* the ground state, with k_1 and k_2 being the apparent decay rate constants of the species A and B, respectively. Please note that the kinetic parameters in Fig. 7 are different from those shown in Table 4. The difference results from different alloxazine and transient concentrations, as the values of Table 4 were obtained by extrapolation to zero alloxazine concentration and low excitation energies, while those of Fig. 7 are raw experimental results corresponding to real alloxazine concentrations and excitation energies.

We also performed triplet state calculations, obtaining $T_1 \rightarrow T_i$ transition energies and oscillator strengths; see Table 3 and Fig. 4. The lowest excited triplet state has the π,π^* character in all of the compounds examined. The T–T excitation energies and transition intensities are shown in Table 3. The predicted visible transitions, located at about $21 \times 10^3\,cm^{-1}$, $25 \times 10^3\,cm^{-1}$, $28 \times 10^3\,cm^{-1}$, and $31 \times 10^3\,cm^{-1}$, are blue-shifted relative to the corresponding experimental bands.

4.3. Fluorescence

The absorption and the corrected fluorescence excitation spectra agree well with each other in all of the solvents examined. The fluorescence emission spectra of all of the dimethyl-substituted alloxazines in all of the solvents examined show a single band. The exact position of the band maximum depends on the environment, but is very similar in 1,4-dioxane, 1,2-dichloroethane and acetonitrile, with a red shift in methanol. The fluorescence emission spectra of dimethylalloxazines excited at 355 nm are presented in Fig. 2. As shown in Table 1, the fluorescence emission maximum shows no dependence on the solvent polarity – compare for example the positions of maxima in 1,4-dioxane, 1,2-dichloroethane and acetonitrile – but is sensitive to the solvent ability to form solute–solvent hydrogen bonds, as notable in the 15–25 nm red shift in the emission maximum upon substituting acetonitrile for methanol.

The present paper is devoted to the effect of the methyl substituent upon the spectral and photophysical properties of dimethylalloxazines, and correlation between these properties and the electronic structure of these compounds. A summary of photophysical parameters of these molecules in their singlet states is given in Table 1, including the previously discussed positions of the absorption and emission maxima, fluorescence quantum yields and lifetimes, and the radiative and non-radiative decay constants for the lowest excited singlet state, the latter calculated as $k_r = \phi_F/\tau_F$ and $\Sigma k_{nr} = 1-\phi_F/\tau_F$. The fluorescence decay kinetics of all of the studied compounds in all of the solvents is well described by a single-exponential function. This was confirmed by the usual statistical criteria of "goodness-of-fit", namely reduced χ^2, Durbin–Watson, and ordinary runs.

The interpretation of the photophysical parameters is less straightforward. However, to start the discussion we can refer to our recent study [2] where we have shown that addition of a methyl group at C(7) or C(8) results in a decrease of the quantum yield of fluorescence and a shortening of the fluorescence lifetime, whereas a methyl group at C(6) or C(9) has an opposite effect. The shortest lifetimes are observed for 7MAll and 8MAll due to increases in both radiative and non-radiative rates in comparison to the 6MAll

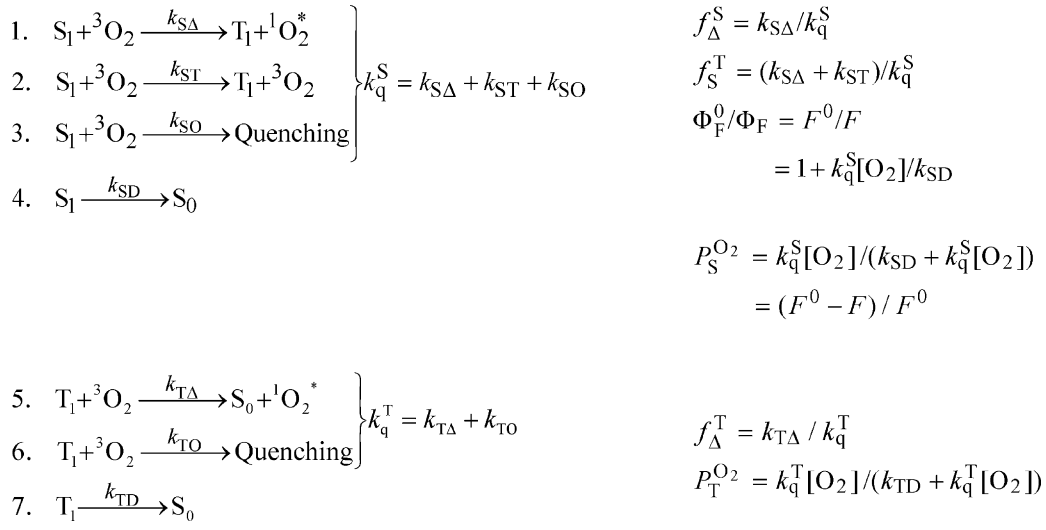

Scheme 1. Fates of electronically excited singlet and triplet states in the presence of molecular oxygen. On the left are indicated the elementary reactions involved, and on the right the various efficiencies derived therefrom. The symbols used are defined in the text.

and 9MAll, which have the longest fluorescence lifetimes in all of the solvents, and correspondingly the lowest radiative and non-radiative excited state decay rates. The data of Table 1 lead to the conclusion that significant substituent effects on the photophysics may be observed in dimethyl-substituted alloxazines. It is very interesting in the context of the above findings to compare 6,9-dimethylalloxazine to 7,8-dimethylalloxazine. The result is, as expected, a very long fluorescence lifetime, but not a very high fluorescence quantum yield, for the 6,9-dimethylalloxazine, and a very short fluorescence lifetime for 7,8-dimethylalloxazine. The result is similar although less spectacular, if we compare photophysical properties of 6,7-dimethylalloxazine, and some other dimethyl-substituted alloxazines, to those of 6,9-dimethylalloxazine. To the best of our knowledge, the fluorescence lifetimes of dimethyl-substituted alloxazines are among the longest ever reported for alloxazines, in some cases, as in 6,9-dimethylalloxazine, the fluorescence lifetime may be even longer than those of a series of structurally related isoalloxazines. However, the non-radiative decay is the dominant path of deactivation in dimethylalloxazines, with the non-radiative rate constant always being much higher than the radiative rate constant, leading to relatively low fluorescence quantum yields. It has to be noted that usually it is assumed that the main difference between iso- and alloxazines is that for alloxazines the fluorescence quantum yield is much lower and the corresponding fluorescence lifetimes much shorter, if compared to isoalloxazines [1]. As can be seen from Table 1, in conjunction with additional data for the fluorescence lifetimes of isoalloxazines [48,65,66], this traditional idea has to be met with some caution, especially as regards the fluorescence lifetimes. The present study also shows that even weak perturbations, such as the introduction of a methyl group or groups, can substantially affect the spectral and photophysical characteristics of alloxazines.

4.4. Singlet oxygen

Considerable interest has been devoted to the ability of a large number of compounds to act as singlet oxygen O_2 ($^1\Delta_g$) photosensitizers, alloxazines being among such potentially interesting compounds. Alloxazines with their relatively strong absorption in the spectral range convenient for excitation are interesting for many reasons. For example, it has been proposed that singlet oxygen produced by different alloxazines may play an important role in the photodegradation of polyamidehydroxyurethane polymers in aqueous solutions [22], and in the photooxidation of substituted phenols in water [67]. However, the amount of data available on alloxazines as singlet oxygen photosensitizers is surprisingly limited, as reflected in the reviews [68,69].

In order to assess the singlet oxygen generating efficiencies of the compounds studied here, we measured the emission at 1270 nm, which is highly specific to the $O_2(^1\Delta_g) \rightarrow O_2(^3\sum g^-)$ transition, under laser excitation at 355 nm of the alloxazines in air-equilibrated acetonitrile solutions. The emission intensity at

Table 5
Effects of H_2O and CH_3CN as bulk solvents on the energies (in 10^3 cm^{-1}) of the lowest excited singlet states by virtue of the conductor polarizable continuum model (CPCM) (the solvent shifts are given in parentheses, differences between the effects of the two solvents never exceeded 100 cm^{-1})

Molecule	Isolated molecule ($\times 10^3$ cm^{-1})	Solvent included[a,b] ($\times 10^3$ cm^{-1})	Solvent included[c] ($\times 10^3$ cm^{-1})	Experimental (in CH_3CN, $\times 10^3$ cm^{-1})
Alloxazine	27.3 n,π*	27.2 (−1.2) π,π*	27.3 (−1.1) π,π*	26.9 π,π*
	28.4 π,π*	28.3 (+1.0) n,π*	28.1 (+0.8) n,π*	
	31.7 n,π*	31.5 (−1.0) π,π*	31.4 (−1.1) π,π*	31.3 π,π*
	32.5 π,π*	33.5 (+1.8) n,π*	32.8 (+1.1) n,π*	
6,9-Dimethylalloxazine	26.2 π,π*	25.4 (−0.8) π,π*	25.4 (−0.8) π,π*	25.8 π,π*
	27.4 n,π*	27.9 (+0.5) n,π*	27.8 (+0.4) n,π*	
	31.1 π,π*	30.4 (−0.7) π,π*	30.3 (−0.8) π,π*	28.8 π,π*
	31.9 n,π*	33.6 (+1.7) n,π*	33.0 (+1.1) n,π*	

[a] Calculated with the ground-state geometry optimized for an isolated molecule.
[b] Compare to the water–6,9-dimethylalloxazine complexes (I–IV, the strongest bound, Table 6): The band 1 (π,π*) at 25.9×10^3 cm^{-1} is shifted to 26.4×10^3 cm^{-1} and the band 2 (π,π*) at 30.6×10^3 cm^{-1} is shifted to 31.3×10^3 cm^{-1}.
[c] Calculated with the ground-state geometry optimized for a molecule in bulk solvent.

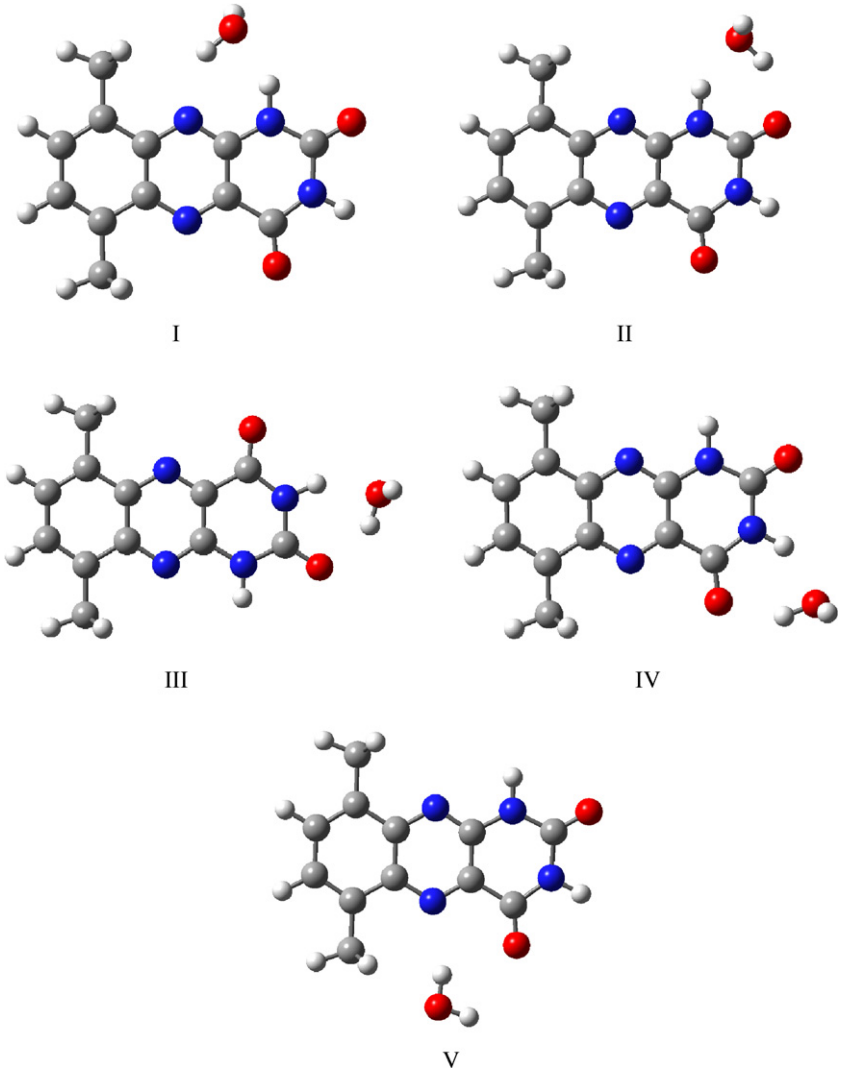

Fig. 8. Possible structures of 6,9-dimethylalloxazine and its complexes with water.

1270 nm increased in samples with higher oxygen concentrations and was extinguished by bubbling N_2 through the solution for a few minutes, demonstrating its origin in singlet oxygen luminescence. In the present work the quantum yields and lifetimes of singlet oxygen, ϕ_Δ and τ_Δ, formed by triplet photosensitization, were determined by exciting air-saturated alloxazine solutions in acetonitrile at 355 nm using perinaphthenone in the same solvent as standard, and are presented in Table 4. The recorded emission lifetimes are typical for singlet oxygen acetonitrile solutions [70]. All these observations confirm that the alloxazines presently studied act as efficient photosensitizers of singlet oxygen. The high singlet oxygen quantum yields shown in Table 3 are consistent with the observed oxygen quenching rate constant being less than 1/9 of the diffusion-controlled value; indeed, the quenching constants calculated on the basis of the data in Table 4 are in the range of $1.1–1.9 \times 10^9$ dm^3 mol^{-1} s^{-1}, well below the diffusion-controlled rate in acetonitrile of 1.9×10^{10} dm^3 mol^{-1} s^{-1}. This suggests that the majority triplet state quenching pathway is via the energy transfer route, hence the efficiency of singlet oxygen production from the quenching of the triplet excited state f_Δ^T should be large. Such low quenching rate constants result in f_Δ^T approaching 1 for a series of hydrocarbons in acetonitrile [71], and hence the singlet oxygen quantum yield from triplet state quenching approaches the triplet state quantum yield. However, f_Δ^T values of unity have not been observed even when quenching rate constants are well below diffusion control, which can be explained on the basis of charge-transfer mediated quenching without energy transfer. Studies have suggested partial charge transfer in acetonitrile during oxygen quenching of excited triplet states of about 11%, for a range of aromatic hydrocarbons and biphenyl derivatives [71]. The various possible interactions between the excited singlet and triplet states and oxygen are illustrated in Scheme 1, with f_Δ^S and f_Δ^T being the efficiencies of singlet oxygen production following quenching by oxygen of the first excited singlet and triplet states, respectively, and $P_S^{O_2}$ and $P_T^{O_2}$ the respective fractions of singlet and triplet states quenched by oxygen.

In the case of alloxazines, the singlet lifetimes are sufficiently short that oxygen quenching under these conditions is expected to be very inefficient. In a previous report regarding alloxazines in acetonitrile [18], we performed some experiments with higher concentrations of oxygen to obtain the rate constant for quenching of the singlet excited states of the alloxazines by oxygen in acetonitrile. On the basis of the rates of singlet state quenching reported there, even in the case of 6,9-dimethylalloxazine in methanol we may only expect to quench around 7% of the excited singlet states. It should be noted, however, that on the basis of the

Table 6
Calculated singlet excitation energies for 6,9-dimethylalloxazine taking into account the bulk solvent effects (acetonitrile and water) by virtue of the CPCM model and calculated singlet excitation energies for the complexes of 6,9-dimethylalloxazine with water I–V

$S_0 \rightarrow S_i$	6,9MAll water		6,9MAll acetonitrile		Complex I		Complex II		Complex III		Complex IV		Complex V	
	$E(\times 10^{-3}\,cm^{-1})$	f	$E(\times 10^{-3}\,cm^{-1})$	f	$E(\times 10^{-3}\,cm^{-1})$	f	$E(\times 10^{-3}\,cm^{-1})$	f	$E(\times 10^{-3}\,cm^{-1})$	f	$E(\times 10^{-3}\,cm^{-1})$	f	$E(\times 10^{-3}\,cm^{-1})$	f
$\rightarrow S_1$	25.4	0.042	25.4	0.042	26.2	0.037	26.0	0.031	26.4	0.031	25.9	0.031	24.7	0.030
$\rightarrow S_2$	27.9	0.002	27.8	0.002	27.4	0.001	27.2	0.001	27.2	0.001	27.5	0.001	27.3	0.0
$\rightarrow S_3$	30.4	0.245	30.4	0.245	30.6	0.165	31.0	0.147	31.3	0.160	30.8	0.172	27.7	0.001
$\rightarrow S_4$	33.5	0.0	33.5	0.0	31.1	0.001	32.1	0.0	31.5	0.0	32.4	0.0	30.6	0.146
$\rightarrow S_5$	38.2	0.414	38.2	0.425	37.2	0.010	38.6	0.333	38.0	0.033	37.5	0.0	32.8	0.0
$\rightarrow S_6$	39.4	0.116	39.5	0.114	37.4	0.0	38.8	0.001	38.8	0.0	38.0	0.015	38.2	0.365
$\rightarrow S_7$	39.9	0.0	39.8	0.0	39.0	0.325	39.7	0.086	39.3	0.011	38.9	0.362	39.0	0.0
$\rightarrow S_8$	40.7	0.0	40.7	0.0	39.5	0.001	40.2	0.0	39.4	0.444	39.4	0.0	39.0	0.008
$\rightarrow S_9$	41.0	0.0	40.9	0.0	40.9	0.002	40.4	0.0	41.0	0.0	40.5	0.0	39.8	0.001
$\rightarrow S_{10}$	42.3	0.277	42.3	0.261	42.0	0.146	42.5	0.123	42.6	0.100	42.2	0.002	40.0	0.012
$\rightarrow S_{11}$	42.5	0.290	42.6	0.303	43.4	0.394	43.4	0.408	43.5	0.021	42.3	0.080	40.5	0.0
$\rightarrow S_{12}$	46.4	0.116	46.4	0.117	43.5	0.010	44.2	0.003	44.0	0.329	43.3	0.452	42.3	0.058
$\rightarrow S_{13}$	46.8	0.0	46.7	0.0	43.7	0.001	45.0	0.0	44.4	0.004	45.2	0.0	42.9	0.407
$\rightarrow S_{14}$	49.8	0.192	49.0	0.0	47.5	0.001	46.9	0.072	47.3	0.061	46.9	0.092	45.5	0.0
$\rightarrow S_{15}$	49.9	0.201	49.8	0.200	47.6	0.076	48.1	0.0	47.6	0.0	48.0	0.0	46.1	0.0

The corresponding oscillator strengths, *f*, are also given.

TD-DFT calculations the separation between the first excited singlet and triplet states for, *e.g.*, 6,7-dimethylalloxazine is close to the energy of singlet oxygen $O_2(^1\Delta_g)$ (97 kJ mol^{-1} as compared to the singlet oxygen energy of 94 kJ mol^{-1}) and hence spin-allowed catalysed intersystem crossing to the triplet state from singlet state quenching with production of singlet oxygen is a theoretical possibility. In the absence of singlet oxygen sensitisation from singlet state quenching, the singlet oxygen quantum yield will equal the triplet state quantum yield if the efficiency of singlet oxygen production from the quenching of the triplet excited state, f_Δ^T, is unity. In such circumstances quantum yield of photosensitized production of singlet oxygen is given by $\phi_\Delta = \phi_{isc} f_\Delta^T P_T^{O_2}$, where ϕ_{isc} is the intersystem crossing quantum yield, $P_T^{O_2}$ is the fraction of the triplet state quenched by O_2 and f_Δ^T is the efficiency of singlet oxygen production, *i.e.*, the fraction of triplet state quenched by oxygen, which gives rise to singlet oxygen. $P_T^{O_2}$ values for these air-saturated acetonitrile solutions depend both on the rate constant of quenching of triplet state by oxygen and on the lifetime of triplet state, and are greater than 0.97 in all cases. On the basis of the data presented, the reported singlet oxygen quantum yields can therefore be regarded as lower estimates of the intersystem crossing yields, demonstrating that the triplet quantum yields are high for these compounds. This observation clearly shows that intersystem crossing rather than internal conversion dominates the non-radiative relaxation rate constants reported in Table 1.

4.5. Solvent effects

The present results obtained in the macroscopic approach using the CPCM model reveal some changes to the predicted singlet ($S_0 \rightarrow S_i$) excitation energies of two alloxazines studied, alloxazine and 6,9-dimethylalloxazine. As typical for alloxazines, there are two pairs of closely located n,π* and π,π* transitions in the lowest-energy part of the spectrum, corresponding to the two experimentally observed absorption bands. The results shown in Table 5 demonstrate that an increase in the polarizability of the environment causes a reduction of the energy of π,π* transitions, and a growth of the energy of n,π* transitions. This causes changes in the order of the lowest excited states in alloxazine, and an increased spacing between the π,π* and n,π* transitions in each pair, in 6,9-dimethylalloxazine.

The results obtained using the microscopic approach used a simplified solvent model with a single water molecule, which should be sufficient to reveal the fundamental trends. The structures of several complexes between 6,9-dimethylalloxazine and water (I–V), as obtained at the B3LYP/6-31G(d) level of theory, are presented in Fig. 8. Table 6 presents the predicted transition energies and oscillator strengths. Binding energies of the complexes of 6,9-dimethylalloxazine with water were also calculated and are listed in Table 7. As can be seen from Table 5, the indirect effect of the solvent (altering the ground-state equilibrium structure of a molecule) is generally one order of magnitude smaller than the direct effect on the energies of the electronic excited states.

The order of transitions is similar to that predicted by the CPCM model, with two pairs of π,π* and n,π* closely-spaced transitions for all of the complexes examined. The electronic energy gap between the S_1 and S_2 states is relatively small, with the highest values corresponding to the complex V (2.6×10^3 cm^{-1}), see Table 6. However, those highest-gap complexes also have the lowest binding energy, of 8.6 kcal/mol. Note that all of the predicted binding energies of 6,9-dimethylalloxazine with water are similar to those predicted for lumichrome – methanol complexes and lumichrome – acetic acid complexes using the same theoretical approach [13].

A water molecule may act both as a hydrogen donor and acceptor agent, thus, the 6,9-dimethylalloxazine–water complexes may have

Table 7
The binding energies and hydrogen bond data of the complexes of 6,9-dimethylalloxazine with water (I–V)

Complex	D–H···A	D–H distance (Å)	H···A distance (Å)	D···A distance (Å)	D–H···A angle (°)	Total energy (hartree)	Binding energy (kcal/mol)
I	N1–H1···O	1.030	1.880	2.810	149	−909.2543277	11.9
	O–H···N10	0.980	2.010	2.870	145		
II	N1–H1···O	1.030	1.880	2.790	145	−909.2563098	13.2
	O–H···O2	0.981	1.940	2.800	146		
III	N3–H3···O	1.031	1.930	2.810	147	−909.2552669	12.5
	O–H···O2	0.980	1.950	2.800	145		
IV	N3–H3···O	1.032	1.890	2.810	146	−909.255635	12.7
	O–H···O4	0.980	1.940	2.790	145		
V	O–H···N5	0.970	2.230	3.180	166	−909.2490823	8.6
	O–H···O4	0.960	2.580	2.980	105		

Note: The DFT total energies of individual molecules were 6,9MAll = −832.8263789 hartree and H_2O = −76.408953 hartree.

various structures. In choosing the structures of the complexes, special attention was given to the possible interactions of water with the active centers of 6,9-dimethylalloxazine, namely N(1)–H, N(3)–H, N(10), and N(5), and both carbonyl oxygens. The present DFT calculations predict that the spectrally suitable complex I is quite feasible, as its calculated binding energy is virtually equal to the binding energies of other complexes, given the typical precision estimate of such calculations of a few kcal/mol, see Table 7. Direct comparison of the DFT calculations with the experiments is not trivial, as the situation in real solvents should be quite complex. Complexes of other than 1:1 stoichiometry may be formed; additionally, both 6,9-dimethylalloxazine and water may produce various aggregates between identical molecules. Nevertheless, it is interesting to compare our theoretical results with the situation in real solvents.

Considering the data presented in Table 7, we can note a correlation between the binding energy and geometry of a single *isolated* hydrogen bond D–H···A. Of the three bond parameters, the D···A distance and the D–H···A angle are particularly indicative of the hydrogen bond strength. However, it is worth noting that in the present complexes, the water molecule is involved simultaneously in two hydrogen bonds, being simultaneously a donor and an acceptor of hydrogen. These two hydrogen bonds should be equally important and, therefore, the observed D–H···A angles result from the equilibrium geometry of the respective complexes. Thus, the presently observable correlations may not coincide with those observed for single hydrogen bonds.

The effect of hydrogen bond formation between 6,9-dimethylalloxazine and a single water molecule upon the spectral properties is of mixed nature, as the resulting transition energies may evolve both towards and away from the experimental values. Therefore, a more complete approach should involve specific interactions with several water molecules, properly averaged, and should account for the bulk of the solvent using CPCM or an equivalent approach. On the other hand, the current error margins of the energy calculations may make such a comprehensive program largely pointless.

5. Conclusions and outlook

The spectral and photophysical properties of the presently studied substituted alloxazines clearly indicate the value of this set of compounds for future comparative studies, including, for example, molecules with very similar structures and different order of n,π* and π,π* excited states, different excited state lifetimes, with their properties modulated by solvents, and having some structural barriers. This set of molecules, comprehensively characterized in four representative solvents, will be used in a number of future studies, including singlet oxygen photosensitization and ESDPT reactions.

Acknowledgments

Grant No. N N204 2659 33 for the years 2007–2010 from the MNiSW, Poland, is gratefully acknowledged. We are also pleased to recognize the generous support extended by the Poznań Supercomputing and Networking Centre.

References

[1] P.F. Heelis, Chem. Soc. Rev. 11 (1982) 15–39.
[2] E. Sikorska, I.V. Khmelinskii, J.L. Bourdelande, A. Bednarek, S.L. Williams, M. Patel, D.R. Worrall, J. Koput, M. Sikorski, Chem. Phys. 301 (2004) 95–103.
[3] E. Sikorska, I.V. Khmelinskii, W. Prukala, S.L. Williams, D.R. Worrall, J.L. Bourdelande, A. Bednarek, J. Koput, M. Sikorski, J. Mol. Struct. 689 (2004) 121–126.
[4] E. Sikorska, I.V. Khmelinskii, A. Bednarek, S.L. Williams, D.R. Worrall, R.J. Herance, J.L. Bourdelande, G. Nowacka, J. Koput, M. Sikorski, Pol. J. Chem. 78 (2004) 2163–2173.
[5] E. Sikorska, I.V. Khmelinskii, S.L. Williams, D.R. Worrall, R.J. Herance, J.L. Bourdelande, J. Koput, M. Sikorski, J. Mol. Struct. 697 (2004) 199–205.
[6] E. Sikorska, H. Szymusiak, I.V. Khmelinskii, A. Koziolowa, J. Spanget-Larsen, M. Sikorski, J. Photochem. Photobiol. A 158 (2003) 45–53.
[7] A. Koziolowa, Photochem. Photobiol. 29 (1979) 459–471.
[8] P.S. Song, M. Sun, A. Koziolowa, J. Koziol, J. Am. Chem. Soc. 96 (1974) 4319–4323.
[9] A. Koziolowa, A.J.W.G. Visser, J. Koziol, Photochem. Photobiol. 48 (1988) 7–11.
[10] E. Sikorska, A. Koziolowa, J. Photochem. Photobiol. A 95 (1996) 215–221.
[11] E. Sikorska, A. Koziolowa, M. Sikorski, A. Siemiarczuk, J. Photochem. Photobiol. A 157 (2003) 5–14.
[12] E. Sikorska, I.V. Khmelinskii, M. Kubicki, W. Prukala, M. Hoffmann, I.F. Machado, L.F.V. Ferreira, J. Karolczak, D.R. Worrall, A. Krawczyk, M. Insinska-Rak, M. Sikorski, J. Phys. Chem. A 110 (2006) 4638–4648.
[13] E. Sikorska, I.V. Khmelinskii, M. Kubicki, W. Prukala, G. Nowacka, A. Siemiarczuk, J. Koput, L.F.V. Ferreira, M. Sikorski, J. Phys. Chem. A 109 (2005) 1785–1794.
[14] E. Sikorska, I.V. Khmelinskii, M. Hoffmann, I.F. Machado, L.F.V. Ferreira, K. Dobek, J. Karolczak, A. Krawczyk, M. Insinska-Rak, M. Sikorski, J. Phys. Chem. A 109 (2005) 11707–11714.
[15] S. Tsukamoto, H. Kato, H. Hirota, N. Fusetani, Biol. Ascidians (2001) 335–340.
[16] S. Tsukamoto, H. Kato, H. Hirota, N. Fusetani, Eur. J. Biochem. 264 (1999) 785–789.
[17] D.A. Phillips, C.M. Joseph, G.P. Yang, E. Martinez-Romero, J.R. Sanborn, H. Volpin, Proc. Natl. Acad. Sci. U.S.A. 96 (1999) 12275–12280.
[18] E. Sikorska, M. Sikorski, R.P. Steer, F. Wilkinson, D.R. Worrall, J. Chem. Soc., Faraday Trans. 94 (1998) 2347–2353.
[19] M. Sikorski, E. Sikorska, A. Koziolowa, R. Gonzalez-Moreno, J.L. Bourdelande, R.P. Steer, F. Wilkinson, J. Photochem. Photobiol. B 60 (2001) 114–119.
[20] M. Sikorski, E. Sikorska, R. Gonzalez-Moreno, J.L. Bourdelande, D.R. Worrall, J. Photochem. Photobiol. A 149 (2002) 39–44.
[21] Z.W. Wang, C.J. Rizzo, Org. Lett. 2 (2000) 227–230.
[22] A. Onu, M. Palamaru, E. Tutovan, C. Ciobanu, Polym. Degrad. Stabil. 60 (1998) 465–470.
[23] A.J. Robak, B.P. Branchaud, Tetrahedron Lett. 46 (2005) 5651–5654.
[24] Z. Miskolczy, L. Biczok, Chem. Phys. Lett. 411 (2005) 238–242.
[25] G. Porcal, S.G. Bertolotti, C.M. Previtali, M.V. Encinas, Phys. Chem. Chem. Phys. 5 (2003) 4123–4128.
[26] M.V. Encinas, S.G. Bertolotti, C.M. Previtali, Helv. Chim. Acta 85 (2002) 1427–1438.
[27] F. Corbin, Int. J. Hematol. 76 (2002) 253–257.
[28] F. Corbin, Bus. Briefing Med. Dev. Manuf. Technol. (2002) 1–3.
[29] Y.H. Zen, C.M. Wang. J. Chem. Soc., Chem. Commun. (1994) 2625–2626.
[30] E. Sikorska, I.V. Khmelinskii, D.R. Worrall, S.L. Williams, R. Gonzalez-Moreno, J.L. Bourdelande, J. Koput, M. Sikorski, J. Photochem. Photobiol. A 162 (2004) 193–201.
[31] E. Sikorska, I.V. Khmelinskii, D.R. Worrall, J. Koput, M. Sikorski, J. Fluorescence 14 (2004) 57–64.

[32] M. Sikorski, E. Sikorska, I.V. Khmelinskii, R. Gonzalez-Moreno, J.L. Bourdelande, A. Siemiarczuk, J. Photochem. Photobiol. A 156 (2003) 267–271.
[33] M. Sikorski, E. Sikorska, I.V. Khmelinskii, R. Gonzalez-Moreno, J.L. Bourdelande, A. Siemiarczuk, in: S.K. Chapman, R.N. Perham, N.S. Scrutton (Eds.), Flavins and Flavoproteins, Rudolf Weber Agency for Scientific Publications, Berlin, 2002, pp. 731–736.
[34] M. Sikorski, E. Sikorska, I.V. Khmelinskii, R. Gonzalez-Moreno, J.L. Bourdelande, A. Siemiarczuk, Photochem. Photobiol. Sci. 1 (2002) 715–720.
[35] M. Sikorski, K. Nakano, E. Sikorska, F. Wilkinson, in: A. Koziolowa, B. Laczkowski, A. Sobczynski, W. Zmudzinski (Eds.), Quality for the XXIst Century, Poznan University of Economics Press, Poznan, 1999, pp. 967–972.
[36] M. Sikorski, E. Sikorska, F. Wilkinson, R.P. Steer, Can. J. Chem.-Revue Canadienne de Chimie 77 (1999) 472–480.
[37] M. Mir, E. Sikorska, M. Sikorski, F. Wilkinson, J. Chem. Soc., Perkin Trans. 2 (1997) 1095–1098.
[38] M. Sikorski, Phys. Chem. Chem. Phys. 4 (2002) 211–215.
[39] M.M. Szafran, J. Koziol, P.F. Heelis, in: B. Curti, S. Ronchi, G. Zanetti (Eds.), Flavins and Flavoproteins, Walter de Gruyter & Co., Berlin/New York, 1991, pp. 41–44.
[40] M.D. Eidiger, R.S. Moog, S.G. Boxer, M.P. Fayer, Chem. Phys. Lett. 88 (1983) 123.
[41] R. Schmidt, C. Tanielian, R. Dunsbach, C. Wolff, J. Photochem. Photobiol. A 79 (1994) 11–17.
[42] E. Gross, J. Dobson, M. Petersilka, Top. Curr. Chem. 181 (1996) 81–172.
[43] A.D. Becke, J. Chem. Phys. 98 (1993) 5648–5652.
[44] R. Ditchfield, W.J. Hehre, J.A. Pople, J. Chem. Phys. 54 (1971) 724–728.
[45] V. Barone, M. Cossi, J. Phys. Chem. A 102 (1998) 1995–2001.
[46] M.J. Frisch, G.W. Trucks, H.B. Schlegel, G.E. Scuseria, M.A. Robb, J.R. Cheeseman, A.J.Jr Montgomery, T. Vreven, K.N. Kudin, J.C. Burant, J.M. Millam, S.S. Iyengar, J. Tomasi, V. Barone, B. Mennucci, M. Cossi, G. Scalmani, N. Rega, G.A. Petersson, H. Nakatsuji, M. Hada, M. Ehara, K. Toyota, R. Fukuda, J. Hasegawa, M. Ishida, T. Nakajima, Y. Honda, O. Kitao, H. Nakai, M. Klene, X. Li, J.E. Knox, H.P. Hratchian, J.B. Cross, V. Bakken, C. Adamo, J. Jaramillo, R. Gomperts, R.E. Stratmann, O. Yazyev, A.J. Austin, R. Cammi, C. Pomelli, J.W. Ochterski, P.Y. Ayala, K. Morokuma, G.A. Voth, P. Salvador, J.J. Dannenberg, V.G. Zakrzewski, S. Dapprich, A.D. Daniels, M.C. Strain, O. Farkas, D.K. Malick, A.D. Rabuck, K. Raghavachari, J.B. Foresman, J.V. Ortiz, Q. Cui, A.G. Baboul, S. Clifford, J. Cioslowski, B.B. Stefanov, G. Liu, A. Liashenko, P. Piskorz, I. Komaromi, R.L. Martin, D.J. Fox, T. Keith, M.A. Al-Laham, C.Y. Peng, A. Nanayakkara, M. Challacombe, P.M.W. Gill, B. Johnson, W. Chen, M.W. Wong, C. Gonzalez, J.A. Pople, Gaussian 03, Revision D.01, Gaussian, Inc., Wallingford, CT, 2004.
[47] E. Sikorska, I.V. Khmelinskii, W. Prukala, S.L. Williams, M. Patel, D.R. Worrall, J.L. Bourdelande, J. Koput, M. Sikorski, J. Phys. Chem. A 108 (2004) 1501–1508.
[48] M. Kowalczyk, E. Sikorska, I.V. Khmelinskii, J. Komasa, M. Insinska-Rak, M. Sikorski, J. Mol. Struct. (Theochem.) 756 (2005) 47–54.
[49] M. Sun, T.A. Moore, P.S. Song, J. Am. Chem. Soc. 94 (1972) 1730–1740.
[50] E. Sikorska, A. Koziolowa, Stud. Commodity Sci. Chem. Z. 210 (1993) 79–87.
[51] C. Neiss, P. Saalfrank, M. Parac, S. Grimme, J. Phys. Chem. A 107 (2003) 140–147.
[52] C.B. Martin, X.F. Shi, M.L. Tsao, D. Karweik, J. Brooke, C.M. Hadad, M.S. Platz, J. Phys. Chem. B 106 (2002) 10263–10271.
[53] C.B. Martin, M.L. Tsao, C.M. Hadad, M.S. Platz, J. Am. Chem. Soc. 124 (2002) 7226–7234.
[54] J. Rodriguez-Otero, E. Martinez-Nunez, A. Pena-Gallego, S.A. Vazquez, J. Org. Chem. 67 (2002) 6347–6352.
[55] C. Neiss, P. Saalfrank, Photochem. Photobiol. 77 (2003) 101–109.
[56] R.J. Platenkamp, M.H. Palmer, A.J.W.G. Visser, Eur. Biophys. J. 14 (1987) 393–402.
[57] Personal communications.
[58] J.K. Eweg, F. Muller, H. Vandam, A. Terpstra, A. Oskam, J. Am. Chem. Soc. 102 (1980) 51–61.
[59] J.K. Eweg, F. Muller, D. Bebelaar, J.D.W. Vanvoorst, Photochem. Photobiol. 31 (1980) 435–443.
[60] J.K. Ewerg, F. Muller, A.J.W.G. Visser, C. Veeger, D. Bebelaar, J.D.W. van Voorst, Photochem. Photobiol. 30 (1979) 463–471.
[61] E.C. Lim, J. Phys. Chem. 90 (1986) 6770–6777.
[62] F.M. Sikorski, F.E. Sikorska, F.D.R. Worrall, F.F. Wilkinson, Internet Photochem. Photobiol. (1998), http://www.photobiology.com/v1/sikorski/index.htm.
[63] E. Sikorska, J.L. Bourdelande, D.R. Worrall, M. Sikorski, Pol. J. Chem. 77 (2003) 65–73.
[64] H. Li, Z.Q. Jiang, Y. Pan, S.Q. Yu, Res. Chem. Int. 32 (2006) 695–708.
[65] E. Sikorska, I.V. Khmelinskii, J. Koput, M. Sikorski, J. Mol. Struct. (Theochem.) 676 (2004) 155–160.
[66] E. Sikorska, I.V. Khmelinskii, J. Koput, J.L. Bourdelande, M. Sikorski, J. Mol. Struct. 697 (2004) 137–141.
[67] K. Tatsumi, H. Ichikawa, S. Wada, J. Contam. Hydrol. 9 (1992) 207–219.
[68] R.W. Redmond, J.N. Gamlin, Photochem. Photobiol. 70 (1999) 391–475.
[69] F. Wilkinson, W.P. Helman, A.B. Ross, J. Phys. Chem. Ref. Data 22 (1993) 113–262.
[70] F. Wilkinson, W.P. Helman, A.B. Ross, J. Phys. Chem. Ref. Data 24 (1995) 663–1021.
[71] A.A. Abdel-Shafi, D.R. Worrall, J. Photochem. Photobiol. A 172 (2005) 170–179.